Tetrahedron Letters xxx (xxxx) xxx

Contents lists available at ScienceDirect

Tetrahedron Letters

journal homepage: www.elsevier.com/locate/tetlet

Synthesis and properties of triphenylamine functionalized tetrathiafulvalene

Xia Tian[a], Fang Qian[b], Min Wu[a], Xiaozhong Liang[a], Fang Zhang[a], Da Li[a], Kunpeng Guo[a,*], Zhike Liu[b,*], Jie Li[a,*]

[a] Ministry of Education Key Laboratory of Interface Science and Engineering in Advanced Materials, Research Center of Advanced Materials Science and Technology, Taiyuan University of Technology, Taiyuan 030024, China
[b] School of Materials Science and Engineering, Shaanxi Normal University, Xi'an 710119, China

ARTICLE INFO

Article history:
Received 15 February 2020
Revised 31 March 2020
Accepted 14 April 2020
Available online xxxx

Keywords:
Tetrathiafulvalene
Triphenylamine
Chemical synthesis
Hole transporting material

ABSTRACT

A hybrid conjugated molecule **TTPA-TTF** was designed and synthesized by combing a tetrathiafulvalene core with *tetra*-triphenylamine derivative functionalized at the 4,4′,5,5′- positions. Studies revealed **TTPA-TTF** exhibits good thermal stability and hole mobility. To explore its primary application as hole-transporting material in perovskite solar cells, **TTPA-TTF** -based cells exhibited a power conversion efficiency of 10.95% without the use of any p-type dopants.

Introduction

Since the pioneering work on "organic metal" based tetrathiafulvalene-tetracyanoquinodimethane (TTF-TCNQ) reported by Ferraris *et al.* in 1973, many studies have focused on design and synthesis of tetrathiafulvalene (TTF) derivatives due to its strong electron-donating ability and polytropic chemical structure [1–5]. In the past decades, charge-transfer systems, magnetic compounds and photovoltaics based on TTF derivatives have attracted great interest due to their unique solid-state properties [6–12]. In these contexts, versatile TTF derivatives have been developed, including replacement of sulfur by other chalcogen atoms, peripheral functionalization of the TTF core, and insertion of conjugated spacers between the dithiafulventl units [13–16]. Among them, the peripheral functionalization of the TTF core with conjugated substituents would be an intriguing way not only to expand π-conjugation system, but also to achieve novel functions [17–20]. Therefore, peripheral groups functionalized TTF derivatives should be explored with altered aromatic groups, especially those containing heteroatoms, for their next applications.

In heteroatom-containing aromatic derivatives, triphenylamine (TPA) derivatives have been extensively studied because of their excellent electronic donating ability and hole-transporting capability, as well as three-dimensional molecular structures [21–25]. For example, spirotype molecule 2,2′,7,7′-tetrakis[*N,N-di*(4-*methoxyphenyl*)*amino*]-9,9′-spirobifluorene (SpiroOMeTAD) adopts a spirobifluorene core with four bis(4-methoxyphenyl)amine substituted at the 2,2′,7,7′- postions represented the most successful commercial hole transporting material (HTM). Perovskite solar cells (PSCs) based on SpiroOMeTAD with the use of p-type dopants have shown the record power conversion efficiencies (PCEs) above 20% [26–28]. However, PSCs based dopant-free SpiroOMeTADT often show poor PCEs below 10% [29–32]. It is well known that dopant-free HTMs not only simplify the devices preparation process, but also improve the stability of the devices. Notably, some researches demonstrated replacing the spirobifluorene core in SpiroOMeTAD with other heteroatom containing aromatic compounds would be efficiency in molecular design toward dopant-free HTMs [33–35]. Therefore, these researches arouse our interests in the functionalization of TTF with TPA-based peripheral groups for novel functions. Motivated by this, we designed a molecule **TTPA-TTF** which feature four TPA derivatives functionalized to a TTF core at its 4,4′,5,5′- positions. We describe here the synthesis and optical, electrochemical, thermal properties of **TTPA-TTF** and its primary application as dopant-free HTM in PSCs.

Results and discussion

The synthetic route for compound **TTPA-TTF** was depicted in Scheme 1. Compound **2** was prepared under a Barbier reaction

---

* Corresponding authors.
E-mail addresses: guokunpeng@tyut.edu.cn (K. Guo), zhike2015@snnu.edu.cn (Z. Liu), lijie01@tyut.edu.cn (J. Li).

https://doi.org/10.1016/j.tetlet.2020.151949
0040-4039/© 2020 Elsevier Ltd. All rights reserved.

Please cite this article as: X. Tian, F. Qian, M. Wu et al., Synthesis and properties of triphenylamine functionalized tetrathiafulvalene, Tetrahedron Letters, https://doi.org/10.1016/j.tetlet.2020.151949

according to the literature method [36]. Chlorine-hydroxyl exchange by reaction of compound **2** and cyanuric chloride to produce compound **3**. Ethanone **3** was converted to **4** by the reaction with potassium *o*-isopropyl xanthate, which was treated with 30% HBr/AcOH to give 1,3-dithiole-2-ketone derivative **5**. Notably, it is no need to change the ketone **5** to a 1,3-dithiole-2-thione derivative, Horner-Wittig coupling reaction of ketone **5** in the presence of triethylphosphite also proceeded to give bromide TTF derivative **6**. Eventually, Buchwald-Hartwig amination of compound **6** and 4,4′-dimethoxydiphenylamine in the presence of tetrakis(triphenylphosphine)palladium and sodium *tert*-butoxide afforded the target compound **TTPA-TTF**. The structures of the compounds were confirmed by NMR and mass spectroscopy characterizations. **TTPA-TTF** showed good solubility in common organic solvents such as dichloromethane, tetrahydrofuran (THF), toluene, and chlorobenzene.

To understand the configuration and frontier molecular orbital distributions of **TTPA-TTF**, theoretical calculations using the Gaussian 09 program at the B3LYP/6-31G* level were performed. As shown in Fig. 1, the centered TTF unit presented a π-conjugated planar structure. The dihedral angles between the peripheral TPA groups and the centered TTF were in the range of 45°–47° for **TTPA-TTF**, indicating the compound exhibited a twisted configuration. The nonplanar molecular structure of **TTPA-TTF** endows it good solubility in common organic solvents, which is beneficial for its practicability for solution-processed organic electronic materials. The electron distributions of the highest occupied molecular orbital (HOMO) of **TTPA-TTF** was mainly localized on the TTF center, while the lowest unoccupied molecular orbital (LUMO) just slightly shifted from TTF unit to the adjacent phenyl rings. This result indicates the donor character of the molecule is mainly stems from the TTF unit.

The absorption spectrum of **TTPA-TTF** in dilute chlorobenzene at room temperature is shown in Fig. 2a. It was observed **TTPA-TTF** exhibits two relatively strong absorption bands in the 300–400 nm region, which can be attributed to a more localized π-π^* in peripheral TPA rings and centered TTF. Compared to its solution, the maximum absorption wavelength of **TTPA-TTF** in film was still < 400 nm, indicating its high transparency to visible light (Fig. S1). The little red-shifted absorption in film relative to its solution spectra was attributed to the possible formation of aggregates. To explore its electrochemical property, the molecular orbital energy levels of **TTPA-TTF** were obtained from the cyclic voltammetry (CV) measurement in combination with the optical band gap (E_g) determined by its absorption onset in solution. It can be found that the E_g of **TTPA-TTF** was 2.25 eV, as shown in Fig. 2a. As illustrated in Fig. 2b, the first oxidation peak of **TTPA-TTF** was observed at 0.91 V. As a result, the HOMO level of **TTPA-TTF** was calculated accordingly as −5.25 eV [34]. The LUMO level of **TTPA-TTF**, calculated as HOMO + E_g, was −3.00 eV. It is noted that the HOMO level of **TTPA-TTF** was higher than the valence band (VB) of perovskite $CH_3NH_3PbI_3$ (−5.43 eV), indicating the hole injection from $CH_3NH_3PbI_3$ to the **TTPA-TTF** is feasible. In addition, its LUMO level is higher than the conduction band (CB) of $CH_3NH_3PbI_3$ (−3.91 eV). Based on this result, the energy barrier of 0.91 eV between the CB of $CH_3NH_3PbI_3$ and the LUMO level of **TTPA-TTF** would block the electrons efficiently from perovskites to the metal electrodes and thus reduce the charge recombination in the perovskites/HTM interface.

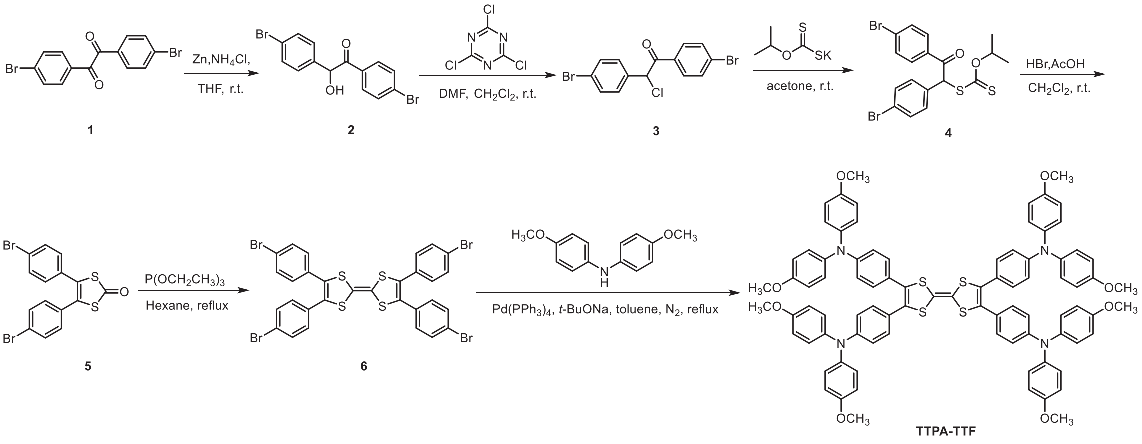

Scheme 1. Synthesis of **TTPA-TTF**.

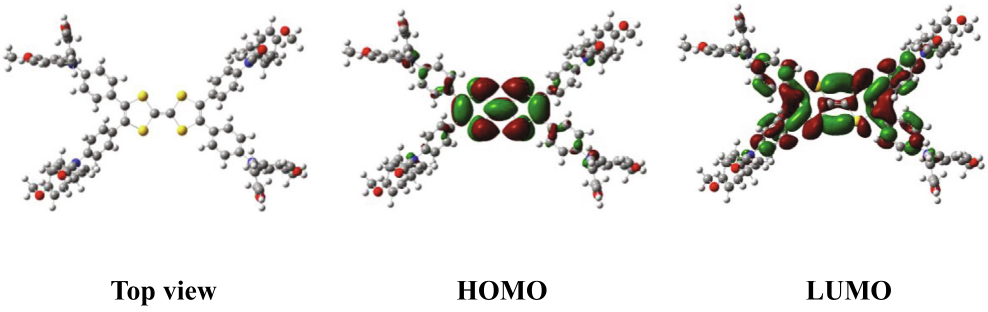

Fig. 1. Optimized structure and the spatial distribution of the HOMO and LUMO orbitals of **TTPA-TTF**.

Please cite this article as: X. Tian, F. Qian, M. Wu et al., Synthesis and properties of triphenylamine functionalized tetrathiafulvalene, Tetrahedron Letters, https://doi.org/10.1016/j.tetlet.2020.151949

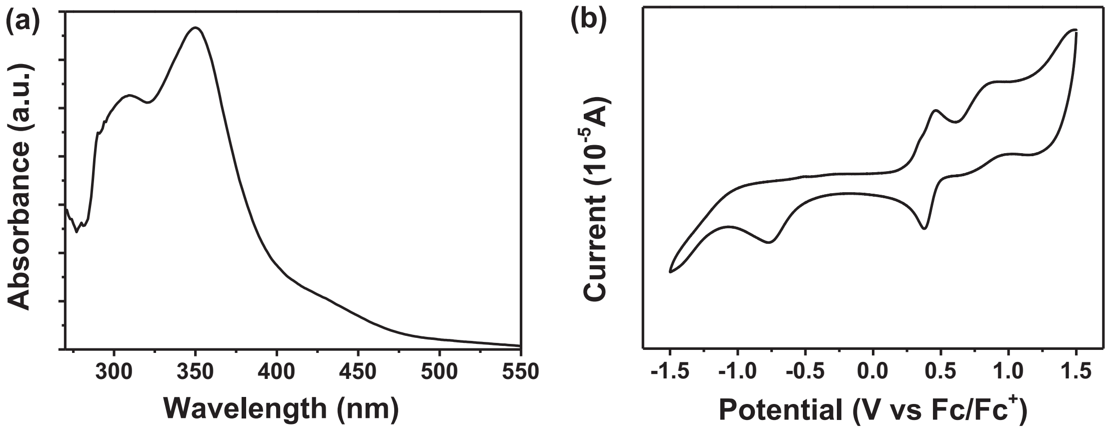

Fig. 2. (a) UV–vis absorption spectrum and (b) cyclic voltammogram of **TTPA-TTF** in dilute chlorobenzene (1×10^{-5} M).

The thermal property of **TTPA-TTF** was investigated by thermogravimetric (TGA) and different scanning calorimetry (DSC) analyses. As shown in Fig. 3a, **TTPA-TTF** showed good thermal stability with a high decomposition temperature (T_d) of 369.0 °C obtained from the TGA measurement, and an endothermic step at 138.7 °C corresponding to the glass transition temperature (T_g) observed in the DSC curve.

To study the charge-transport property of **TTPA-TTF**, single charge carrier device based on **TTPA-TTF** was fabricated by spin coating its chlorobenzene solution, and the carrier mobility of the compound was calculated using the space charge limited current (SCLC) method. Herein, the structure of the hole-only device was ITO/PEDOT: PSS/HTM/MoO_3/Al, where the HTM referred to **TTPA-TTF**. Light emission was not detected from the hole-only devices during the measurement, indicating that the electron is not injected and recombined with the hole. Thus, **TTPA-TTF** exhibited hole-transporting characteristic. The mobility was determined by fitting the dark current to the model of a single carrier SCLC, which was

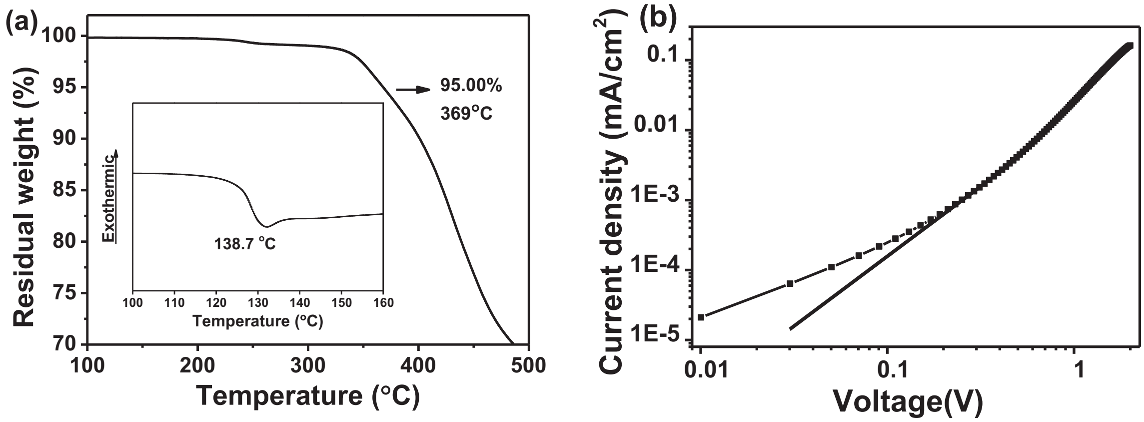

Fig. 3. (a) TGA and DSC (inset) curves of **TTPA-TTF**. (b) J-V curve of hole only device with an architecture of ITO/PEDOT: PSS/**TTPA-TTF** /MoO_3/Al.

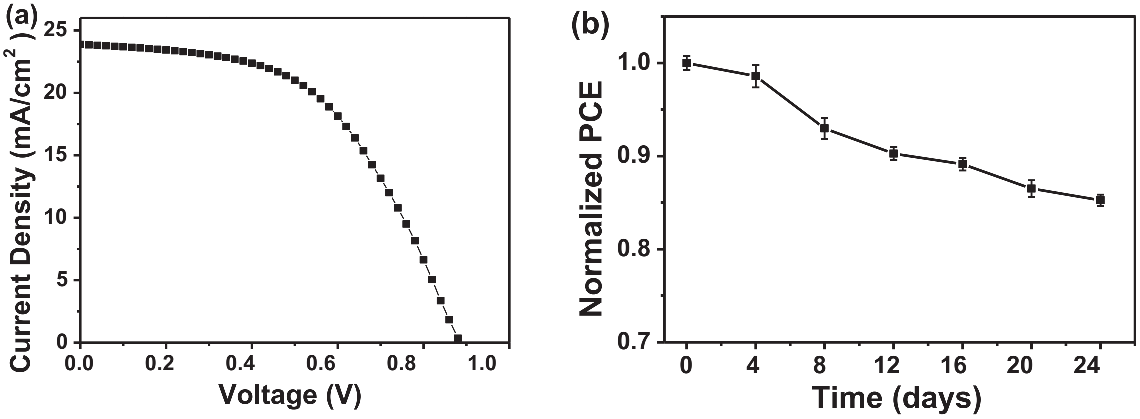

Fig. 4. (a) Current density–voltage curve of one of the best performing devices using undoped **TTPA-TTF** as HTM. (b) Stability test of undoped **TTPA-TTF** based PSCs.

Please cite this article as: X. Tian, F. Qian, M. Wu et al., Synthesis and properties of triphenylamine functionalized tetrathiafulvalene, Tetrahedron Letters, https://doi.org/10.1016/j.tetlet.2020.151949

described by the Mott–Gurney law. As shown in Fig. 3b, the **TTPA-TTF** exhibits a high hole-mobility of 1.06×10^{-4} cm^2 V^{-1} S^{-1}.

The suitable energy levels, high thermal stability and hole-mobility suggested **TTPA-TTF** could be developed as a dopant-free HTM for PSCs. With these in mind, a PSC structured of FTO/TiO_2/$CH_3NH_3PbI_3$ / **TTPA-TTF** /Au without any p-type dopants was assembled and tested. The photovoltaic performances of the PCS were measured under AM1.5G (100 $mWcm^{-2}$) irradiation, and the current density–voltage (*J-V*) curve is displayed in Fig. 4(a). The device based on **TTPA-TTF** displayed a short-circuit density (J_{sc}) of 23.88 mA cm^{-2}, an open circuit voltage (V_{oc}) of 0.88 V, and a fill factor (*FF*) of 0.52, thus giving a PCE of 10.95%. Fig. S2 showed statistics data on the reproducibility of the PSCs performance. The average PCEs for 40 devices based on **TTPA-TTF** were 9.61 ± 0.84%, which indicated good reproducibility of the devices. Furtherly, to explore the durability of the photovoltaic performance of the PSCs based on **TTPA-TTF,** the PCE change with time of unencapsulated device by storing them in air with a relative humidity of 30% was investigated (Fig. 4b). After aging for 24 days, the **TTPA-TTF**-based PSC retained 85.2% of its initial PCE, indicating good stability of the device.

Conclusion

In summary, to explore the properties and application of the heteroatom-containing aromatic groups functionalized TTF derivatives, a new TTF-centered, four TPA functionalized molecule **TTPA-TTF** has been synthesized. Studies implied TPA functionalized TTF compound would be promising hole-transporting candidates. As a primary application, the PSC based on the dopant-free **TTPA-TTF** yields a moderate PCE of 10.95% with good stability. This work not only paves a new way for developing peripheral groups functionalized TTFs but also sheds light on the future design of highly efficient HTMs.

Declaration of Competing Interest

The authors declare that they have no known competing financial interests or personal relationships that could have appeared to influence the work reported in this paper.

Acknowledgment

This work was supported by the National Natural Science Foundation of China (NO. 21303117, 61704101).

Appendix A. Supplementary data

Supplementary data to this article can be found online at https://doi.org/10.1016/j.tetlet.2020.151949.

References

[1] Ferraris John, D.O. Cowan, V. Walatka, J.H. Perlstein, J. Am. Chem. Soc. 95 (1973) 948–949.
[2] S. Rabaça, S. Oliveira, A.C. Cerdeira, D. Simão, I.C. Santos, M. Almeida, Tetrahedron Lett. 55 (2014) 6992–6997.
[3] J. Liu, Y. Wu, C. Qin, X. Yang, T. Yasuda, A. Islam, K. Zhang, W. Peng, W. Chen, L. Han, Energy Environ. Sci. 7 (2014) 2963–2967.
[4] V.A. Azov, Tetrahedron Lett. 57 (2016) 5416–5425.
[5] N. Martín, Chem. Commun. 49 (2013) 7025–7027.
[6] B. Xu, H. Chakraborty, R.C. Remsing, M.L. Klein, S. Ren, Adv. Mater. 29 (2017) 1605150.
[7] G. Chen, I. Mahmud, L.N. Dawe, Y. Zhao, Org. Lett. 12 (2010) 4.
[8] Y. Si, G. Yang, Z. Su, J. Mater. Chem. C 1 (2013) 1399.
[9] K. Guo, K. Yan, X. Lu, Y. Qiu, Z. Liu, J. Sun, F. Yan, W. Guo, S. Yang, Org. Lett. 14 (2012) 2214–2217.
[10] F. Pointillart, B. le Guennic, O. Cador, O. Maury, L. Ouahab, Acc. Chem. Res. 48 (2015) 2834–2842.
[11] M. Wu, J. Li, R. Zhang, X. Tian, Z. Han, X. Lu, K. Guo, Z. Liu, Z. Wang, Org. Lett. 20 (2018) 780–783.
[12] L. Jia, G. Zhang, D. Zhang, D. Zhu, Tetrahedron Lett. 51 (2010) 4515–4518.
[13] M.R. Cerón, M. Izquierdo, N. Alegret, J.A. Valdez, A. Rodríguez-Fortea, M.M. Olmstead, A.L. Balch, J.M. Poblet, L. Echegoyen, Chem. Commun. 52 (2016) 64–67.
[14] G.-N. Li, D. Wen, T. Jin, Y. Liao, J.-L. Zuo, X.-Z. You, Tetrahedron Lett. 52 (2011) 675–678.
[15] M. Shao, Y. Zhao, Tetrahedron Lett. 50 (2009) 6897–6900.
[16] J.M. Fabre, Chem. Rev. 104 (2004) 5133–5150.
[17] X. Li, G. Zhang, H. Ma, D. Zhang, J. Li, D. Zhu, J. Am. Chem. Soc. 126 (2004) 11543–11548.
[18] M. Yamashita, H. Hayashi, N. Aratani, H. Yamada, Tetrahedron Lett. 56 (2015) 3804–3808.
[19] M. Yamashita, K. Kawano, A. Matsumoto, N. Aratani, H. Hayashi, M. Suzuki, L. Zhang, A.L. Briseno, H. Yamada, Chem. Eur. J. 23 (2017) 15002–15007.
[20] Nishida J. Naraso, S. Ando, J. Yamaguchi, K. Itaka, H. Koinuma, H. Tada, S. Tokito, Y. Yamashita, J. Am. Chem. Soc. 127 (2005) 10142–10143.
[21] X. Liu, X. Ding, Y. Ren, Y. Yang, Y. Ding, X. Liu, A. Alsaedi, T. Hayat, J. Yao, S. Dai, J. Mater. Chem. C 6 (2018) 12912–12918.
[22] R. Yuan, L. Zhang, L. Chen, H. Zhang, P. Dou, X. Ren, W. Chen, H. Zhou, Y. Wan, H. Wu, Tetrahedron Lett. 60 (2019) 1803–1807.
[23] G. Wu, Y. Zhang, R. Kaneko, Y. Kojima, K. Sugawa, T.H. Chowdhury, A. Islam, Q. Shen, Md Akhtaruzzaman, T. Noda, J. Otsuki, J. Sol. RRL. 1 (2017) 1700096.
[24] Y.-L. Xu, W.-L. Ding, Z.-Z. Sun, Nanoscale. 10 (2018) 20329–20338.
[25] J. Wang, K. Liu, L. Ma, X. Zhan, Chem. Rev. 116 (2016) 14675–14725.
[26] L.-L. Jiang, Z.-K. Wang, M. Li, C.-H. Li, P.-F. Fang, L.-S. Liao, J. Mater. Chem. A 7 (2019) 3655–3663.
[27] X. Wang, J. Wu, Y. Yang, X. Liu, Q. Guo, Z. Song, G. Li, Z. Lan, M. Huang, J. Mater. Chem. A 7 (2019) 13256–13264.
[28] X. Niu, N. Li, C. Zhu, L. Liu, Y. Zhao, Y. Ge, Y. Chen, Z. Xu, Y. Lu, M. Sui, Y. Li, A. Tarasov, E.A. Goodilin, H. Zhou, Q. Chen, J. Mater. Chem. A 7 (2019) 7338–7346.
[29] X. Zhou, F. Kong, Y. Sun, Y. Huang, X. Zhang, R. Ghadari, Dyes Pigm. 173 (2020) 107954.
[30] S. Paek, P. Qin, Y. Lee, K.T. Cho, P. Gao, G. Grancini, E. Oveisi, P. Gratia, K. Rakstys, S.A. Al-Muhtaseb, C. Ludwig, J. Ko, M.K. Nazeeruddin, Adv. Mater. 29 (2017) 1606555.
[31] S. Ranallo, A. Amodio, A. Idili, A. Porchetta, F. Ricci, Chem. Sci. 7 (2016) 66–71.
[32] J. Lee, M. Malekshahi Byranvand, G. Kang, S.Y. Son, S. Song, G.-W. Kim, T. Park, J. Am. Chem. Soc. 139 (2017) 12175–12181.
[33] X. Yin, J. Zhou, Z. Song, Z. Dong, Q. Bao, N. Shrestha, S.S. Bista, R.J. Ellingson, Y. Yan, W. Tang, Adv. Funct. Mater. 29 (2019) 1904300.
[34] X. Liang, K. Wang, R. Zhang, K. Li, X. Lu, K. Guo, H. Wang, Y. Miao, H. Xu, Z. Wang, Dyes Pigm. 139 (2017) 764–771.
[35] C. Yin, J. Lu, Y. Xu, Y. Yun, K. Wang, J. Li, L. Jiang, J. Sun, A.D. Scully, F. Huang, J. Zhong, J. Wang, Y.-B. Cheng, T. Qin, W. Huang, Adv. Energy Mater. 8 (2018) 1800538.
[36] X.-L. Sun, D.-M. Liu, D. Tian, X.-Y. Zhang, W. Wu, W.-M. Wan, Nat. Commun. 8 (2017) 1210.

Please cite this article as: X. Tian, F. Qian, M. Wu et al., Synthesis and properties of triphenylamine functionalized tetrathiafulvalene, Tetrahedron Letters, https://doi.org/10.1016/j.tetlet.2020.151949